16th Australasian Fluid Mechanics Conference
Crown Plaza, Gold Coast, Australia
2-7 December 2007

Characteristics of flow regimes for single plates of rectangular cross-section

A.M. Blazewicz[1], M.K. Bull[1] and R.M. Kelso[1]

[1]School of Mechanical Engineering
University of Adelaide, Adelaide, South Australia, 5005 AUSTRALIA

Abstract

Flow characteristics including velocity fluctuations, acoustic pressure fluctuations and surface pressures have been measured for single plates of rectangular cross section with various chord-to-thickness ratios C and a range of high Reynolds numbers. The flow measurements were complemented with hydrogen-bubble flow visualisation. The results obtained lead to some modification of the flow regimes proposed in the past. Symmetrical modes of vortex shedding, previously observed for the shedding from a circular cylinder, were detected. Frequency components lower than the characteristic shedding frequency were also measured in the flow and acoustic spectra for one of the flow regimes. These components are believed to arise from different types of vortex-corner interaction reported previously for a shear layer impinging on a corner. Results of measurements of separation bubble length for longer plates indicate that for plates shorter than $C \approx 17$ the length of the bubble is influenced by the presence of trailing edges.

Introduction

Details of the flow over rectangular plates and the resulting acoustic radiation are strongly dependent on the chord-to-thickness ratio of a plate, $c/t = C$, and Reynolds number. This investigation focuses on flow at high Reynolds numbers for which a shear layer undergoes laminar-to-turbulent transition immediately after separating from the leading edge of the plate (Nakamura, Ohya and Tsuruta [8]).

Depending on C, the turbulent boundary layers can either roll into a regular vortex street in the wake of the plate without reattachment or with intermittent reattachment on the plate ('short' plates), or permanently reattach to form a separation bubble on the plate streamwise surface ('long' plates). For the short plates there is a critical value of $C \approx 0.6$ below which the plate does not interact with the separated shear layer – Regime 1 (Bearman and Trueman [1]).

Using wake frequencies from peaks in the velocity fluctuation spectra measured by hot-wire sensors for $Re_t = Ut/\nu = (14.8 - 31.1) \times 10^3$ and from flow visualisation, Parker and Welsh [11] identify four different flow regimes, depending on chord-to-thickness ratio. For $C \leq 3.2$, the separated leading-edge shear layers do not reattach to the plate, but interact directly downstream of the trailing edge to form a vortex street (corresponding to Regime 2). In Regime 3 for $3.2 < C \leq 7.6$, intermittent reattachment of the shear layers separated from the leading edge of the plate occurs on the streamwise surfaces. In Regime 4 with $7.6 < C < 16$, permanent reattachment of the shear layer occurs, but no dominant spectral peak is detectable. In Regime 5, $C \geq 16$, reattachment occurs and the spectra show a broad spectral peak that becomes sharper as C increases. Regimes 2 and 3 correspond to "short" plates and Regimes 4 and 5 to long plates. In Regime 4, in which the separated shear layers always reattach to the plate, although Parker and Welsh did not detect any characteristic frequency, weak and irregular trailing-edge vortex shedding has been observed by others.

In their measurements of the frequency of vortex shedding from rectangular plates, Okajima, Mizota and Tanida [10], Nakamura and Nakashima [7] and Nakamura, Ohya and Tsuruta [8] find that as C is increased, stepwise increases in Strouhal number occur at particular values of C (~ 3, 6, 9, 12 etc.). The same effect is evident, to a limited extent, in the results obtained by Parker and Welsh [11] for $C = \sim 1$ - 8. Between steps the Strouhal number $St = ft/U$ based on plate thickness decreases continuously, but the Strouhal number $St_c = fc/U$ based on plate chord is approximately constant.

For 'long' plates with a sufficiently long chord-to-thickness ratios, the length of the separation bubble from the leading edge depends on the state of the separated shear layer, laminar or turbulent, at both separation and reattachment. For Reynolds numbers $Re_t \geq 300$ - 400, a long plate may be taken as one with $C \geq 7$ (Sasaki and Kiya [13]). Extensive experimental investigations of leading-edge-separation bubbles made at higher Reynolds numbers, generally in the range $20\times10^3 \leq Re_t \leq 70\times10^3$, have been reviewed by Kiya [4]. It is concluded that for $C > 7.6$ the separated shear layer always reattaches on the streamwise surface of the plate; the mean length of the separation bubble is generally found to be in the range $4.5t$ to $5.0t$ and independent of Reynolds number. The bubble is not steady, the instantaneous reattachment position fluctuating over a range of typically $0.4x_R$ (or about $2t$).

Experimental Arrangements

In all measurements, conducted at $3.2\times10^3 \leq Re_t \leq 53\times10^3$, the plate arrays were mounted between large end-plates, so that flow over them was nominally two-dimensional. Velocity fluctuations, mean surface pressures, and mean lengths of the separation bubble were measured in an open-jet low-speed wind-tunnel using hot-wire anemometer, surface static-pressure tappings and a differential-pressure surface-fence probe respectively. Acoustic measurements were made in a reverberation chamber. The plate arrays were subjected to the jet flow from a two-dimensional nozzle of the same width as the plates, fed from a compressed-air reservoir. Measurements were made while the pressure in the reservoir was allowed to run down continuously, giving a jet velocity slowly decreasing from about 200 m/s to about 15 m/s. Sound pressure levels were obtained as spatial averages from a condenser microphone traversing the reverberation chamber. Hydrogen-bubble flow visualisation was performed in a water tunnel, giving a maximum Reynolds number $Re_t \approx 3\times10^3$. The differences in Reynolds number affected to some extend the range of C at which a particular flow regime occurred but, in most cases, did not significantly affect the flow pattern. It was therefore assumed that flow patterns at high Reynolds numbers, at which flow and acoustic measurements were conducted, are generally similar to those obtained in the flow visualisation.

Results and Discussion

The range of plate chord ratios investigated covers four of the five characteristic flow regimes identified in the previous investigations. Regime 1 with $C \leq 0.6$, identified by [1], was not investigated. Both acoustic and flow measurements generally confirm the existence of the various regimes, although the values of C which define the limits of the different regimes are, as might

be expected, not precisely the same as established in earlier investigation by Parker & Welsh [11], where measurements were generally conducted in low-speed wind tunnels. In the present work, Regime 4, reported in [11], was not observed. Instead, the present experiments found Regimes 3 and 5 to overlap.

Regime 2

Examples of flow patterns of Regime 2 are shown in figures 1a and b. The plate contours are superimposed on the flow visualisation pictures to indicate an actual plate cross-section at the plane of the hydrogen bubble sheet. Figure 1a shows the flow around a plate with $C = 2$ at $Re_t \approx 800$, with separated shear layers forming a regular von Karman vortex street. However such anti-symmetric vortex shedding occasionally switches into symmetrical shedding as shown in figure 1b. This symmetric mode, also observed at higher Reynolds numbers $Re_t \approx 1300$ and for shorter plates ($C = 1$), appears infrequently and lasts for relatively short periods of time (typically few shedding cycles). Similar bi-stable flow was reported by Unal and Rockwell [14] in flow around a circular cylinder at certain values of Reynolds numbers and cylinder aspect ratios, with the anti-symmetrical flow pattern occurring at least 92 % of time. Norberg [9] observed switching between regular (von Karman) vortex shedding and "irregular flow" in flow around a circular cylinder with end-plates for aspect ratios below 7 at $1360 \leq Re_d \leq 2600$. However the irregular mode was associated with suppression of vortex formation by the critically small end-plates at low aspect ratios. In the current investigation the symmetrical vortex street consists of well-defined vortices.

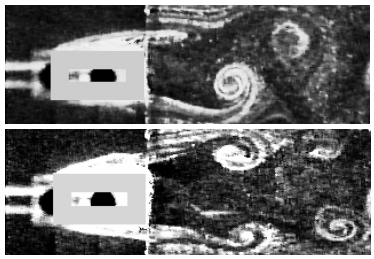

Figure 1. Hydrogen bubble flow visualisation for a plate with $C = 2.0$ at $Re_t \approx 800$: **(a)** anti-symmetric mode and **(b)** symmetrical mode.

In this flow regime, for plates with $1.0 \leq C \leq 3.13$, the Strouhal numbers obtained from the largest peaks in the acoustic spectra St_{2a} have approximately the same value as Strouhal numbers measured from velocity fluctuations St_{2v} (see figure 2). As in the case of the flow spectra, the main acoustic peaks for Regime 2 are accompanied by harmonic peaks (figure 3a). The general agreement between the flow and acoustic Strouhal numbers indicates that the acoustic radiation is predominantly a result of vortex formation in the separated shear layer.

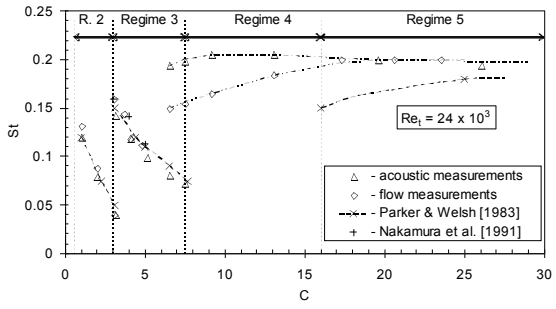

Figure 2. Variation of Strouhal numbers St with chord-to-thickness ratio C for single, rectangular plates.

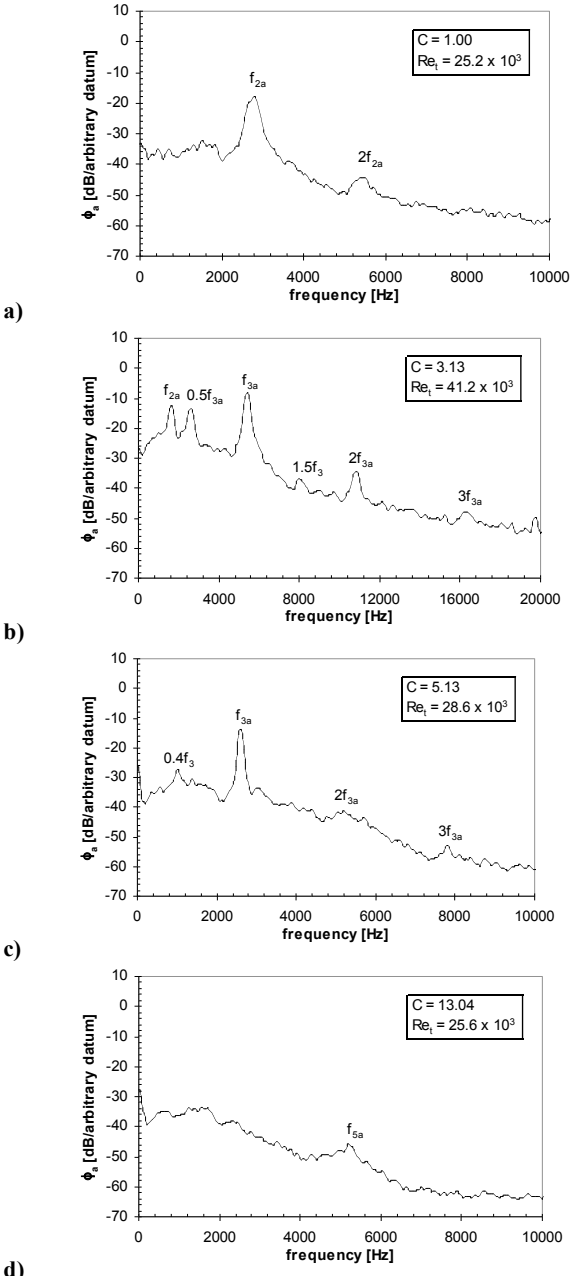

Figure 3. Acoustic frequency spectra ϕ_a for various chord ratios $C = c/t$, and Reynolds numbers $Re_t = Ut/\nu$.

The existence of the various regimes is further confirmed by base pressure measurements. The variation of base pressure coefficient Cp_b with C over the range $1 \leq C < 20$ at one particular Reynolds number $Re_t = 16.5 \times 10^3$ is shown in figure 4. The character of the relationship changes at the values of C associated with the limits of the different flow regimes.

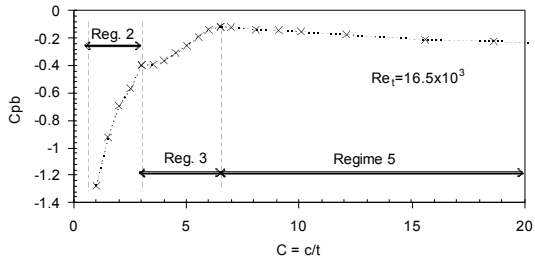

Figure 4. Variation of base pressure coefficient Cp_b with chord-to-thickness ratio C.

Regime 3

A typical flow pattern of Regime 3 at $Re_t \approx 600$ is shown in figure 5 for a plate with $C = 3.6$. In this case the separated shear layers reattach intermittently on the streamwise surfaces of the plates, as is indicated by hydrogen bubbles swept downstream from a wire located just downstream of the plate's trailing edge (top streamwise surface in figure 5). The separated shear layer on the other side of the plate rolls up downstream of the trailing edge without reattachment, as indicated by hydrogen bubbles being entrained upstream between the separated shear layer and the plate streamwise surface (bottom streamwise surface in figure 9). The shear layers from both sides of the plates merge downstream of the trailing edges and form von Karman vortex street.

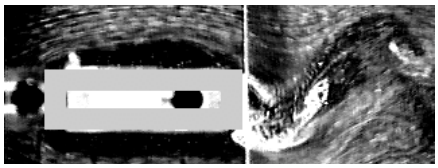

Figure 5. Hydrogen bubble flow visualisation at $Re_t \approx 600$ for a plate with $C = 3.6$.

The Strouhal numbers St_{3a} obtained from the largest peaks in the acoustic spectra have similar values to Strouhal numbers St_{3v} obtained from velocity spectra. The peaks are distinct and accompanied by harmonics for the lower values of C (as for C = 5.13, figure 3c), but become smaller and less distinct as C is increased. Acoustic spectral peaks at f_{3a} were detected up to C = 9.65. For the plate with $C = 3.13$ both St_{2a} and St_{3a} are present (figure 3b). Similarly, in the flow measurements for the plate with $C = 3.05$, peaks at both St_{2v} and St_{3v} were detected also. These results indicate that in this C range the flow is bistable and can switch from Regime 2 to Regime 3.

The acoustic spectra exhibit a number of distinct peaks that consistently appear over certain velocity ranges. Similar although less distinct peaks have also been detected in the velocity-fluctuation spectra. For the plates with $C = 3.13$ (figure 3b) peaks at frequencies equal to 0.5 f_{3a} are clearly visible and they are accompanied by less distinct peaks at $1.5f_{3a}$. The acoustic spectra for $4.13 \le C \le 9.65$ show peaks at frequencies of approximately $0.4f_{3a}$ ($C = 5.13$, figure 3c). The spectra for C = 6.52 and 7.52 (not shown) and 7.52 show peaks at frequencies roughly equal (0.6 - 0.7)f_{3a} and $1.7f_{3a}$.

Similar low-frequency components and their non-linear interactions with fundamental frequencies were observed by Knisely and Rockwell [6] in the pressure and velocity fluctuations of a separated shear layer impinging on a corner. The low-frequency components, which could have amplitudes of the same order as the fundamental frequency (β), were associated with the variation in impingement location of successive vortices arising from the amplified instability wave. Four possible vortex-corner interactions were observed by Rockwell and Knisely [12]. The ordered cycling between the classes of interaction gave rise to the low-frequency components. In the case of shorter distances between the separation and impingement of the shear layer on the corner, persistent cycling between two classes of interaction produced a low-frequency component at 0.5β. For larger distances between the separation and reattachment, a more complex pattern of cycling was observed, producing components at 0.2β, 0.4β, 0.6β and 0.8β. It is believed that the low-frequency components detected in the acoustic and velocity-fluctuation spectra of the present Regime 2 flow are produced by a similar type of interaction involving cycling between different classes of vortex-corner interaction.

The weakening of the characteristic peaks with the increase of C may indicate that as the time during which the separated shear layer is reattached to the plate increases the vortex formation in the layer becomes weaker and less regular and the flow becomes dominated by complex, three-dimensional flow fluctuations in the separated shear layers, as reported in previous investigations such as Kiya and Sasaki [5].

Regime 5

Figure 6 shows flow in Regime 5 around a plate with $C = 10$ at $Re_t \approx 600$ where the shear layers separate at the leading edges and reattach on the plate's streamwise surfaces, forming permanent separation bubbles. The streak lines visible in the figure 6 never reach the plate surface, with the mean separation/reattachment streamline located under the streak lines. The reattached flow separates at the trailing edges of the plate, forming a periodic vortex street. At higher Reynolds numbers a similar flow pattern is observed, except that the shear layers separating at the leading edges undergo turbulent transition near reattachment. It is expected that for higher Reynolds numbers the laminar-turbulent transition would move upstream until it reaches the leading edge, with the trailing edge shedding still present.

Figure 6. Hydrogen bubble flow visualisation for a plate with $C = 10.0$, $Re_t \approx 600$.

In this regime the only characteristic discrete frequency associated with vortex shedding in the shear layer, corresponding Strouhal number St_{5v}, was detected in the flow downstream of the plate trailing edge. Similarly, the acoustic spectra have a small but distinct peak at frequency f_{5a} and a corresponding St_{5a}. The peak, broad and indistinct, first appears for the plate with C = 6.52, becomes larger as C is increased to 13.04 (figure 3d), and remains approximately unchanged with further increase in C. As in the velocity-fluctuation spectra, the peak is broader and not as well defined as the peaks in Regime 2 or those for smaller C in Regime 3.

In contrast to the findings for Regimes 2 and 3, it is apparent in figure 2, that there is a considerable difference between the values of St_{5v} and St_{5a}, particularly for small C, even though the Strouhal number values tend to converge as C is increased. This difference can be explained by different flow conditions such as blockage ratio, flow uniformity, free-stream turbulence intensity and compressibility effects, and by three-dimensional effects such as boundary layer thickness at the side walls of the rig.

In the acoustic measurements for plates with $6.52 \le C \le 9.65$, where there is evidence of an overlap of Regimes 3 and 5, spectra corresponding to this plate range, shown in figure 3b for $C = 3.13$, show peaks at characteristic frequencies associated with Regime 3 (f_{3a}) and Regime 2 (f_{2a}).

Measurements of the mean separation bubble length $X_R = x_R/t$ as a function of C, presented in figure 7 for $18.2 \times 10^3 \le Re_t \le 52.8 \times 10^3$, indicate that for plates shorter than $C \approx 17$ the length of the bubble is influenced by the presence of the trailing edges with X_R increasing with C. For sufficiently long plates ($C > 17$) X_R becomes constant. The value of X_R obtained in the present work ($X_R \approx 6.0$ - 6.2, depending on Reynolds number) is significantly higher than those obtained in previous experiments and summarised by Djilali and Gartshore [3] ($4.5 \le X_R \le 5.5$). The discrepancy can be associated with the different experimental conditions: even though the two sets of data were obtained at low free-stream turbulence, the previous data were collected in closed working sections while present data have been obtained in the semi-open jet. The general trend of the previous results, with X_R increasing as blockage ratio decreases, indicates that the present results are believable. Another source of the discrepancy can be related to different aspect ratios. In

the current results the plate aspect ratio (defined as a ratio of plate span to plate thickness) is 17.5 which is in most cases larger than the aspect ratios of the data summarised by Djilali and Gartshore [3]. According to the data presented by Cherry *et al.* [2] the length of the separation bubble increases with the plate aspect ratio. The current data also show a slight dependence on Reynolds number for the Reynolds number as high as $Re_t \approx 53 \times 10^3$ (figure 7). Similar behaviour was observed by Cherry et al. [2] who showed that the separation bubble decreased in length due to the shortening of the laminar part of shear layer with increasing Reynolds number. However, this behaviour was only detected for $Re_t < 30 \times 10^3$.

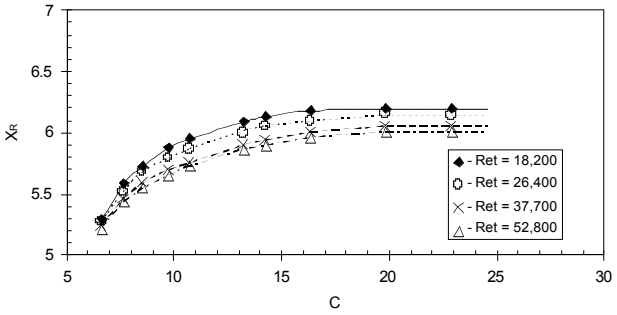

Figure 7. Variation of separation bubble length X_R with chord-to-thickness ratio C.

Conclusions

The following conclusions concerning flow around rectangular plates with $1.0 \le C \le 68.0$ can be drawn:

1. Of the five regimes of variation of Strouhal number with chord-to-thickness ratio which have been identified in the previous research, only three occur over the range of C and Re_t of this investigation. Regime 4, reported by Parker and Welsh [11], was not observed. Regime 1 was not covered in the present range of chord to thickness ratios.

2. In **Regime 2**, which can exist for $1.0 \le C \le 3.13$, and in which the separated shear layers roll up to form a vortex street downstream of the trailing edge of the plate without reattachment to it, there is a strong correspondence between the Strouhal numbers of the velocity fluctuations and the Strouhal numbers of frequency peaks observed in acoustic spectra. This leads to the conclusion that the vortex formation in the separated shear layer is the main cause of noise radiation. The level of acoustic radiation reaches its maximum value at C corresponding to longer plates within this range.

The anti-symmetric vortex street, which is a characteristic flow pattern for this regime, can occasionally, for a duration of a few shedding cycles, switch into a symmetric shedding mode, at least for $Re_t \le 1300$.

3. In **Regime 3**, which can exist for $3.05 \le C \le 9.65$, and in which the separated shear layers reattach intermittently to the streamwise plate surfaces, vortex formation in the shear layer is the dominant cause of noise radiation for the smaller chord-to-thickness ratios. As the chord-to-thickness ratio is increased, the vortex shedding becomes weaker and the magnitude of the radiated noise drops as it apparently becomes dominated by complex three-dimensional effects. The radiation is also influenced by the low-frequency components associated with a variation in the impingement location of successive vortices and, for the chord-to-thickness ratio of $6.52 \le C \le 9.65$, bistable flow switching between Regimes 3 and 5.

4. In **Regime 5**, which can exist for $6.52 \le C \le 68$ (and probably for larger C), and in which the separated shear layer reattaches to the streamwise plate surfaces forming a permanent separation bubble, the only vortex shedding with a detectable discrete frequency appears to occur at the trailing edge of the plate. This trailing-edge vortex shedding is weak and irregular, especially for the plates with the smaller chord-to-thickness ratios. It contributes to the noise radiation, but sound power level of the spectral peak corresponding to the shedding is relatively low.

The mean length of the separation bubble formed on the plate becomes independent of chord length only for relatively long plates ($C > 17$). The bubble length is also to some extent dependent on the flow Reynolds number and experimental conditions. The values of the mean bubble length obtained in the present experiment are 22 % higher than those obtained in previous experiments in closed-type working sections. This difference is attributed to blockage and model aspect ratios.

5. Bistable behaviour of the flow over the plates, with apparently random switching between the flow regimes, occurs for $C \approx 3$ between Regime 2 and Regime 3, and $6.52 \le C \le 9.65$ between Regime 3 and Regime 5. This is evident in both acoustic and flow data.

References

[1] Bearman P.W. and Trueman D.M., An investigation of the flow around rectangular cylinders. *Aero. Q.*, **23**, 1972, 229-237.

[2] Cherry N.J., Hillier R. and Latour M.E.M.P., Unsteady measurements in a separated and reattaching flow. *J. Fluid Mech.*, **144**, 1984, 13-46.

[3] Djilali N. and Gartshore I.S., Turbulent flow around a bluff rectangular plate. Part I: Experimental investigation. *J. Fluids Eng.,* **113**, 1991, 51-59.

[4] Kiya M., Separation bubbles. *Theoretical and Applied Mechanics*, Elsevier Science Publishers B.V., 1989. 173-191.

[5] Kiya M. and Sasaki K., Structure of a turbulent separation bubble. *J. Fluid Mech.*, **137**, 1983, 83-113.

[6] Knisely C. and Rockwell D., Self-sustained low-frequency components in an impinging shear layer. *J. Fluid Mech.*, **116**, 1982, 157-186.

[7] Nakamura Y. and Nakashima M., Vortex excitation of prisms with elongated rectangular, H and | cross-sections. *J. Fluid Mech.*, **163**, 1986, 149-169.

[8] Nakamura Y., Ohya Y. and Tsuruta H., Experiments on vortex shedding from flat plates with square leading and trailing edges. *J. Fluid Mech.,* **222**, 1991, 437-447.

[9] Norberg C., An experimental investigation of the flow around a circular cylinder: influence of aspect ratio. *J. Fluid Mech.*, **258**, 1994, 287-316.

[10] Okajima A., Mizota T. and Tanida Y., Observations of flow around rectangular cylinders. *3rd International Symp. of Flow Visualisation*, Michigan, 1983, 381-386.

[11] Parker R. and Welsh M.C., Effects of sound on flow separation from blunt flat plates. *Int. J. Heat and Fluid Flow,* **4(2)**, 1983, 113-127.

[12] Rockwell D.O. and Knisely C., Vortex-edge interaction: Mechanics for generating low frequency components. *Phys. Fluids*, **23(2)**, 1980, 239-240.

[13] Sasaki K. and Kiya M., Three-dimensional vortex structure in a leading-edge separation bubble at moderate Reynolds numbers. *J. Fluids Eng.,* **113**, 1991, 405-410.

[14] Unal M.F. and Rockwell D., On vortex formation from a cylinder. Part 1. The initial instability. *J. Fluid Mech.,* 190, 1988, 491-512.